JCTC Journal of Chemical Theory and Computation

Article

pubs.acs.org/JCTC

Raman Spectra of Liquid Water from *Ab Initio* Molecular Dynamics: Vibrational Signatures of Charge Fluctuations in the Hydrogen Bond Network

Quan Wan,[†] Leonardo Spanu,[†] Giulia A. Galli,*[,†,‡] and François Gygi[§]

[†]Department of Chemistry, University of California, Davis, California 95616, United States,

[‡]Department of Physics, University of California, Davis, California 95616, United States, and

[§]Department of Computer Science, University of California, Davis, California 95616, United States

Supporting Information

ABSTRACT: We report the first *ab initio* simulations of the Raman spectra of liquid water, obtained by combining first principles molecular dynamics and density functional perturbation theory. Our computed spectra are in good agreement with experiments, especially in the low frequency region. We also describe a systematic strategy to analyze the Raman intensities, which is of general applicability to molecular solids and liquids, and it is based on maximally localized Wannier functions and effective molecular polarizabilities. Our analysis revealed the presence of intermolecular charge fluctuations accompanying the hydrogen bond (HB) stretching modes at 270 cm^{-1}, in spite of the absence of any Raman activity in the isotropic spectrum. We also found that charge fluctuations partly contribute to the 200 cm^{-1} peak in the anisotropic spectrum, thus providing insight into the controversial origin of such peak. Our results highlighted the importance of taking into account electronic effects in interpreting the Raman spectra of liquid water and the key role of charge fluctuations within the HB network; they also pointed at the inaccuracies of models using constant molecular polarizabilities to describe the Raman response of liquid water.

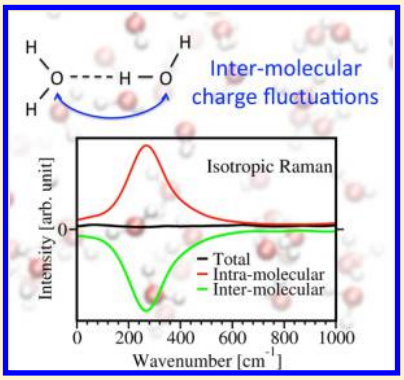

INTRODUCTION

Vibrational spectroscopy is widely used as a probe of the structure and dynamics of water and aqueous solutions in various environments.[1,2] In particular, Raman spectroscopy was extensively employed to investigate the O−H stretching band[3−8] and low-frequency translational and librational bands[4,9−17] of liquid water at ambient conditions and under pressure,[18−21] as well as the vibrational properties of solvated ions[22−25] and biological molecules[26,27] in solutions, and of nanoconfined water.[28,29]

Most of the theoretical studies carried out to interpret the measured Raman spectra of water are currently based on classical simulations,[26,30−38] with Raman intensities computed from the time-correlation function (TCF) of the polarizability tensor.[39] The latter is obtained from molecular polarizabilities either derived empirically or calculated from small water clusters using *ab initio* electronic structure methods. In principle, quantum TCFs are required for an accurate description of the vibrational excitations. However, in most simulations[26,30−35] quantum TCFs are approximated with classical ones, and then multiplied by a so-called quantum correction factor.[40] The authors of refs 35−38 proposed a method to compute quantum TCFs within a semiclassical approximation, encompassing the generation of trajectories using classical molecular dynamics (MD) and the calculation of Raman intensities of clusters extracted from MD trajectories. These calculations yielded very good agreement with experiments, but they were restricted to the analysis of the O−H stretching band. Overall, while some theoretical studies found good agreement with experiments for the Raman activities of the O−H stretching band,[37,38] most results for the low-frequency part of the Raman spectra were not as satisfactory,[26,30−32,34] and a number of open questions remain in the interpretation of the Raman spectra of liquid water at ambient condition.

In particular, the origin of the low-frequency bands at 60 cm^{-1} and 200 cm^{-1} are not fully understood,[41−43] and their interpretation calls for the use of ab initio calculations, where electrons are treated explicitly. As pointed out in the case of infrared (IR) spectra,[44−46] it is important to properly account for dynamical changes in the electronic structure of water molecules and of the HB network to accurately describe the vibrational properties of the liquid.

In this paper, we report the first *ab initio* simulation of the Raman spectra of liquid water, obtained by using density functional perturbation theory (DFPT).[47] *Ab initio* calculations of Raman spectra based on classical TCF and polarizabilities derived from the modern theory of polarization were so far only reported for crystalline systems,[48,49] but not for liquids. We also developed a systematic strategy to interpret the computed Raman spectra, which is of general applicability to solid and

Received: June 22, 2013
Published: July 24, 2013

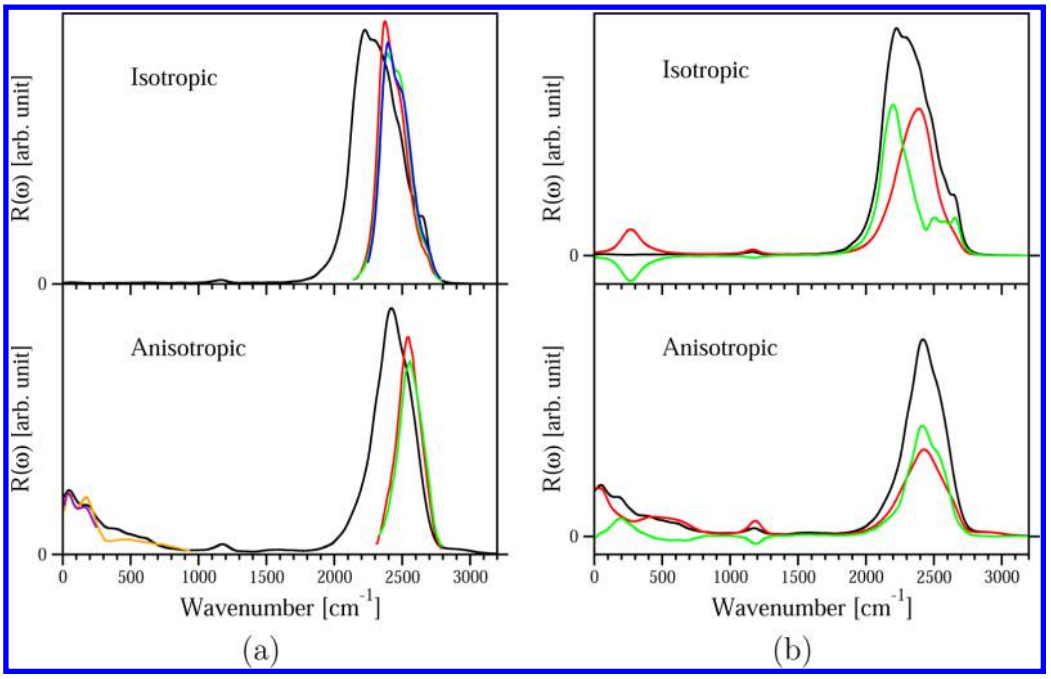

Figure 1. (a) Calculated isotropic (upper panel) and anisotropic (lower panel) Raman spectra (black lines) compared with several experiments. Red, blue and green curves are experimental Raman spectra of heavy water measured at 283 K,[3] 293 K,[6] and 303 K,[3] respectively. Orange and purple curves (below 1000 cm^{-1}) show experimental Raman spectra of hydrogenated water at 278 K and 308 K.[10] (b) Calculated isotropic (upper panel) and anisotropic (lower panel) Raman spectra (black lines) decomposed into intra- (red lines) and inter- (green lines) molecular contributions.

liquid phases of molecular systems. Our analysis is based on maximally localized Wannier functions (MLWF),[50] previously used to compute the IR spectrum of liquid water.[44−46,51,52] Our interpretation of the high-frequency O−H stretching band is overall consistent with previous experimental and theoretical studies. In the low-frequency region, our analysis of the isotropic spectrum revealed intermolecular charge fluctuations accompanying HB stretching vibrations, despite the absence of any Raman intensity. Such fluctuations, identified at 200 cm^{-1} in the IR spectrum,[44,53,54] exhibit signals on a wider frequency range in our calculations, up to 270 cm^{-1}. We further defined molecular polarizabilities,[55−58] which may be useful in the parametrization of polarizable force fields for classical MD simulations of water.

The rest of the paper is organized as follows: in the next section, we describe our computational and analysis methods. In the Results and Discussions section, first we compare the calculated Raman spectra with experimental results; we then focus on the interpretation of the low frequency part of the spectrum, and we show evidence of intermolecular charge fluctuations using several complementary analysis tools. Finally, we present our conclusions.

METHODS

We carried out Born−Oppenheimer *ab initio* MD simulations of liquid water using the Qbox code[59] and the semilocal exchange-correlation functional PBE.[60] Based on previous studies with the PBE functional, we used a 64 heavy water sample at the experimental density and an elevated temperature around 400 K, to better reproduce the liquid radial distribution functions and diffusion coefficient.[46,61] We used a plane wave basis set with a kinetic energy cutoff of 85 Ry, norm conserving pseudopotentials[62] of the HSCV type[63] and only the Γ point to sample the Brillouin zone. Our MD simulations were carried out with a time step of 10 au (0.24 fs) in the NVE ensemble for 50 ps after a 5 ps equilibration in the NVT ensemble, using the thermostat proposed in ref 64. We adopted the diagonalization algorithm of ref 65 to compute the MLWFs.[50]

We computed the Raman spectra as the Fourier transform of the TCF of the system's polarizabilities.[39] In this paper, we report the Bose−Einstein reduced[66] isotropic and anisotropic Raman spectra:

$$R_{\mathrm{iso}}(\omega) \propto \frac{\hbar\omega}{kT}\int \mathrm{d}t\ \mathrm{e}^{-i\omega t}\langle \bar{\alpha}(0)\bar{\alpha}(t)\rangle \tag{1}$$

$$R_{\mathrm{aniso}}(\omega) \propto \frac{\hbar\omega}{kT}\int \mathrm{d}t\ \mathrm{e}^{-i\omega t}\left\langle \frac{2}{15}\mathrm{Tr}\beta(0)\beta(t)\right\rangle \tag{2}$$

In eqs 1 and 2, ω is the frequency, Tr denotes a trace operator, T is the temperature and k is the Boltzmann constant. $\bar{\alpha}$ and β are the isotropic and anisotropic components of the polarizability tensor α: $\bar{\alpha} = (1/3)\mathrm{Tr}\alpha$ and $\beta = \alpha - \bar{\alpha}\,\mathbf{I}$, where $\mathbf{I}$ is the identity tensor (see the Supporting Information (SI) for details). The isotropic and anisotropic spectra are an alternative representation of the experimental observable VV and VH spectra (arising from different polarization direction of the incident and the scattered light, either Vertical (V) or Horizontal (H)): $R_{\mathrm{VV}} = R_{\mathrm{iso}} + R_{\mathrm{aniso}}$, $R_{\mathrm{VH}} = 3/4R_{\mathrm{aniso}}$.[39]

We computed the polarizability using density functional perturbation theory (DFPT),[47] as implemented in the Qbox code. In order to understand the contribution of individual water molecules to the total polarizability, we defined the effective molecular polarizability α_i^{eff} of the ith water molecule by projecting the total polarizability α onto MLWFs. The polarization $\mathbf{P}_i$ corresponding to the ith molecule is therefore

$$\mathbf{P}_i = \alpha_i^{\mathrm{eff}}\mathbf{E} \tag{3}$$

where $\alpha = \sum_i \alpha_i^{\mathrm{eff}}$, and $\alpha_i^{\mathrm{eff}} = \sum_c \alpha_{i,c}^{\mathrm{eff}}$; $\alpha_{i,c}^{\mathrm{eff}}$ is the polarizability projected on each of the four MLWFs centers(c) belonging to a water molecule (2 bond pairs and 2 lone pairs MLWFs,

dx.doi.org/10.1021/ct4005307 | J. Chem. Theory Comput. 2013, 9, 4124−4130

constructed from a unitary transformation of valence eigenstates of the Hamiltonian). $\alpha_{i,c}^{\mathrm{eff}}$ is obtained by defining the polarization in terms of MLWF instead of eigenstates. Using the definition of the effective molecular polarizabilities, we further defined intra- and intermolecular contributions to the total Raman spectra, similar to previous IR spectra studies[44−46] (see the SI for details).

Following refs 55−58, we defined the molecular polarizabilities, α_i, of the ith water molecule in the liquid as

$$\mathbf{P}_i = \alpha_i \mathbf{E}_i^{\mathrm{loc}} \tag{4}$$

where $\mathbf{P}_i$ is the molecular polarization of each molecule as defined in eq 3 and $\mathbf{E}_i^{\mathrm{loc}}$ is the local electric field acting on the ith molecule; note that $\mathbf{E}_i^{\mathrm{loc}}$ contains the contribution of both the applied field $\mathbf{E}$ and the field induced by the polarization $\mathbf{P}_j$ ($j \neq i$) of all other molecules in the system via dipole−induced dipole (DID) interactions (see the SI for details). DID interactions[26,31,32,34,35,67] are widely used in classical calculations of Raman spectra to obtain the total polarizability of the extended system from the molecular polarizabilities. In principle, higher multipoles also contributes to E_i^{loc}, but these effects are usually small compared to DID interactions.[68]

We note that α_i^{eff} (eq 3) and α_i (eq 4) are fundamentally different quantities: α_i is an intrinsic molecular property depending solely on the electronic structure of the molecule in the system; that is, if we carved a molecule out of the extended system, keeping its wave functions (and hence MLWFs) and coordinates unchanged, and we placed it in vacuum, its polarizability would be exactly α_i. Instead α_i^{eff} is deduced from the projection of the total polarization onto each molecule. Thus, it contains also induced polarization terms arising from the environment:

$$\alpha_i^{\mathrm{eff}} = \alpha_i + \alpha_i^{\mathrm{DID}} \tag{5}$$

where α_i^{DID} denotes the DID contributions from the environment.

RESULTS AND DISCUSSIONS

Calculated Raman Spectra: Comparison with Experiments. Our calculated isotropic and anisotropic Raman spectra are presented in Figure 1a, together with several experimental results. In the case of the low-frequency anisotropic spectrum, we compared our results with measurements for hydrogenated water, since it has been shown experimentally that the anisotropic spectra of H_2O and D_2O are essentially the same in this region.[16]

As expected, the position of the calculated high-frequency O−D stretching band is red-shifted by about 200 cm^{-1} compared with the experimental band, and it is broader. This error is mainly due to the use of the semilocal functional PBE as discussed in refs 46, 61, and 69 in the case of infrared spectra, where it was shown that the use of the PBE0 functional can greatly improve the description of the position of the water stretching band, as well as its width. The use of some van der Waals functionals (see ref 69) may also lead to an improvement of the position of the band.

There are three main features in the measured isotropic Raman spectrum: two intense peaks at 2400 cm^{-1} and 2500 cm^{-1} and a shoulder in the isotropic spectrum at 2700 cm^{-1}. The intensities of the two peaks vary as a function of temperature from 0 to 100 °C.[3,6] As shown in the upper panel of Figure 1b, our computed spectra also exhibit three main features: we found that the peak at 2200 cm^{-1} arises mainly from intermolecular contributions, while the one at 2400 cm^{-1} has an intramolecular nature. Although the peak positions are red-shifted in our simulations and their separation is overestimated, due to the use of the PBE functional, our results are consistent with experiments and with those of previous studies.[7,37,38,70] In our calculations, the position of the shoulder is in better agreement with experiments than that of the two main peaks; this shoulder is predominantly determined by the vibrations of non-hydrogen-bonded (NHB) species, with both inter- and intramolecular contributions. In the isotropic spectrum, in agreement with experiments,[5] we did not detect any significant signal at frequencies lower than those of the stretching band.

Low-Frequency Bands. In the region below 300 cm^{-1}, the isotropic Raman spectrum (upper panel of Figure 1a) shows no features; the anisotropic spectrum (lower panel) exhibits instead two distinct peaks at 60 cm^{-1} and 200 cm^{-1}, in remarkable agreement with experiments[10] and at variance with previous theoretical studies[26,30−32,34] based on classical models. The slight deviation between theory and experiments (broad band over 300 cm^{-1}) in the librational region is likely due to the different mass of the hydrogen atom in experiments and calculations. The weak peak around 1200 cm^{-1} arises from the water bending mode. The origin of the peaks at 60 cm^{-1} and 200 cm^{-1} has been greatly debated.[41−43] Some studies[4,17,42] assigned the peaks to transverse and longitudinal acoustic modes respectively, others to HB bending and stretching modes.[4,21] Ref 17 related the peak at 60 cm^{-1} to bifurcated HB. Recent *ab initio* simulations of the IR spectrum of liquid water, where two peaks were detected at the same frequencies (although with different intensities), suggested that the 200 cm^{-1} one arises from intermolecular charge fluctuations[44,54] and from the presence of the tetrahedral HB network.[44] It was also suggested that the one at 60 cm^{-1} corresponds to localized vibrations, while the peak at 200 cm^{-1} corresponds to coupling between HB molecules.[45,67]

We analyzed the 60 and 200 cm^{-1} peaks in terms of intra- and intermolecular contributions (Figure 1b) and found that the former comes mainly from intramolecular vibrations, while the latter shows a significant intermolecular contribution, in agreement with previous studies.[45,67] In addition, we found that, at 270 cm^{-1}, positive intra- and negative intermolecular contributions cancel each other (see upper panel of Figure 1b), with the total spectrum showing no significant intensity. This indicates the presence of anticorrelated vibrations on different molecules, which are in antiphase but have the same amplitude. As shown below, such anticorrelation signals the presence of intermolecular charge fluctuations between HB water molecules, consistent with the correlation between the polarizability of the water molecules and the bond order of the HB O−D bond recently reported in ref 57.

In order to identify charge fluctuations, we used the sum of the squared spreads of the MLWFs centered on a given molecule to describe the charge transfer from that molecule to neighboring ones. The spread S_{w_n} of MLWFs is defined as[50]

$$S_{w_n}^2 = \langle w_n | r^2 | w_n \rangle - \langle w_n | \mathbf{r} | w_n \rangle^2 \tag{6}$$

and describes the spatial extension of each MLWFs. To analyze the spectral properties of the charge density, we computed the spread power spectrum and further decomposed it into intra- and intermolecular contributions (see the SI for details), and

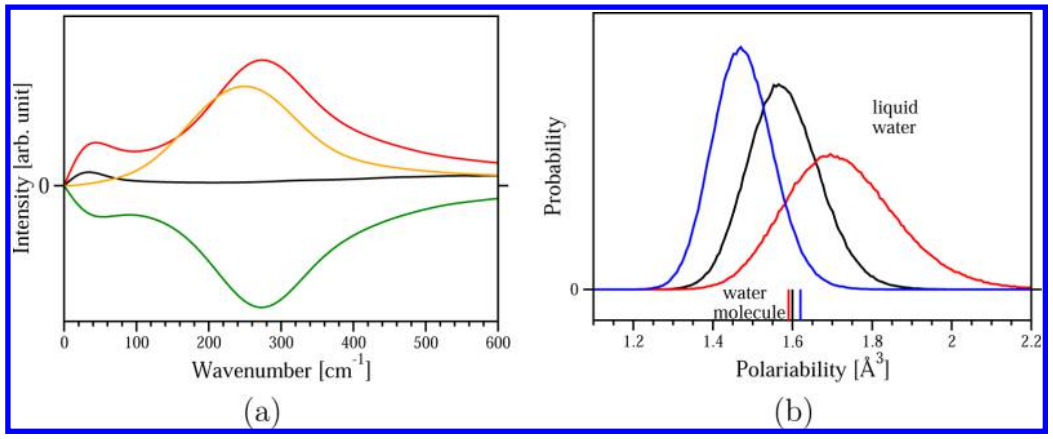

Figure 2. (a) The spectrum (black line) calculated from the spread of the MLWFs (see text) is decomposed into intra- (red line) and inter- (green line) molecular contributions. The vibrational density of states of the relative speed between oxygen atoms of HB water molecules is also shown (orange line). (b) Distribution of different components of the molecular polarizabilities of water molecules obtained in the simulation, compared with the polarizability of an isolated water molecule in different directions (vertical bars): black, red, and blue lines represent polarizabilities along the dipole axis, the axis perpendicular to and the axis within the molecular plane, respectively.

we found the same anticorrelation behavior at 270 cm^{-1} as observed in the isotropic Raman spectrum (Figure 2a).

To understand the origin of the charge fluctuation feature at 270 cm^{-1}, we analyzed the vibrational density of states (VDOS) obtained from the relative speed between the oxygen atoms of HB molecular pairs:

$$I_{\mathrm{VDOS}} = \int \mathrm{d}t\ \mathrm{e}^{-i\omega t} \langle |\mathbf{v}_{\mathrm{O-O}}(0)||\mathbf{v}_{\mathrm{O-O}}(t)| \rangle \qquad (7)$$

Equation 7 includes only the HB stretching vibrational motion, and rotations of water pairs are ignored. As shown in Figure 2a, the resulting spectrum exhibits a peak at 250 cm^{-1}, very close to 270 cm^{-1}, indicating a clear relation between HB stretching and intermolecular charge fluctuations.

In summary, our analysis showed that in liquid water at ambient conditions, intermolecular HB stretching modes, centered at 270 cm^{-1}, are accompanied by intermolecular charge fluctuations. While there is no peak at this frequency in the isotropic Raman spectrum because of the anticorrelation nature of intermolecular charge fluctuations, a peak is present in the anisotropic Raman spectrum and also in the IR spectrum,[44,54] albeit at a slightly lower frequency of 200 cm^{-1}. This difference in frequency is probably caused by different selection rules determining isotropic Raman, anisotropic Raman, and IR spectra. We note that so far the study of charge transfer between water molecules had been restricted to gas-phase molecules and small clusters using either molecular-beam scattering experiments[71] or quantum chemistry calculations.[72−75] Although various studies including classical[54,76] and *ab initio*[44,57] simulations suggested the presence of intermolecular charge fluctuations in liquid water, most classical water models, such as SPCE[77,78] and TIP4P,[79] completely neglected this effect. Only very recently, water models that incorporated charge transfer effects have been reported.[80−82]

Molecular Polarizabilities. We now turn to the analysis of the molecular polarizabilities of water molecules in the liquid.[55,56] We first compare them with the polarizability of water in the gas phase and we then estimate the contribution of molecular polarizabilities to Raman spectra. We then separate and analyze contributions from individual molecules and the environment.

The value of the isotropic molecular polarizability of water molecules, computed as an ensemble average, is 1.60, the same as for an isolated molecule. The experimental value of the molecular polarizability in the liquid is 1.47, again the same as in the gas phase; it was estimated from the measured refraction index n using the Lorentz−Lorenz equation: $(n^2-1)/(n^2+2) = (4\pi/3N)\bar{\alpha}_M$, where N is the number of molecule per unit volume and $\bar{\alpha}_M$ is the isotropic molecular polarizability. Although the calculated values overestimate experiments, due to the use of the PBE functional,[83,84] our results show that the molecular polarizability of water is the same in the liquid and for an isolated molecule, in agreement with experiments and consistent with previous calculations.[56,57]

The distribution of the different components of the α_i tensor computed for liquid water is shown in Figure 2b. The polarizability projected on the molecular dipole axis is the same as in the isolated molecules, while that perpendicular to the molecular plane is significantly enhanced and the one on the in-plane axis decreased. The out-of-plane axis represents the direction least sensitive to the screening of the nuclei, and thus, the polarizability component on this axis is the most affected by the environment,[56] and its distribution is broader. The in-plane component is, instead, smaller than in the gas phase and displays a narrower distribution. This indicates that, not surprisingly, the molecular polarizability of water is more anisotropic in the liquid than in an isolated molecule, consistent with previous classical simulations.[26,33,34] We note that while in qualitative agreement with results reported in the literature,[56,57] the distribution of α_i shown in Figure 2b is broader and the anisotropy is larger compared to previous studies. This is probably due to the use of different functionals (PBE versus BLYP).

We also note that many polarizable force fields adopted in the literature to simulate water (see a description of selected water models, e.g. in ref 85) use a value of the polarizability smaller than the experimental one[86] in order to reproduce structural and diffusive properties of the liquid; in addition, most often it is assumed that the polarizability tensor is isotropic,[87] although models with different polarizability components[88] have been suggested. Hence, no parametrization of existing force fields is consistent with the *ab initio* results reported here and in previous first principles studies.[56,57] Our

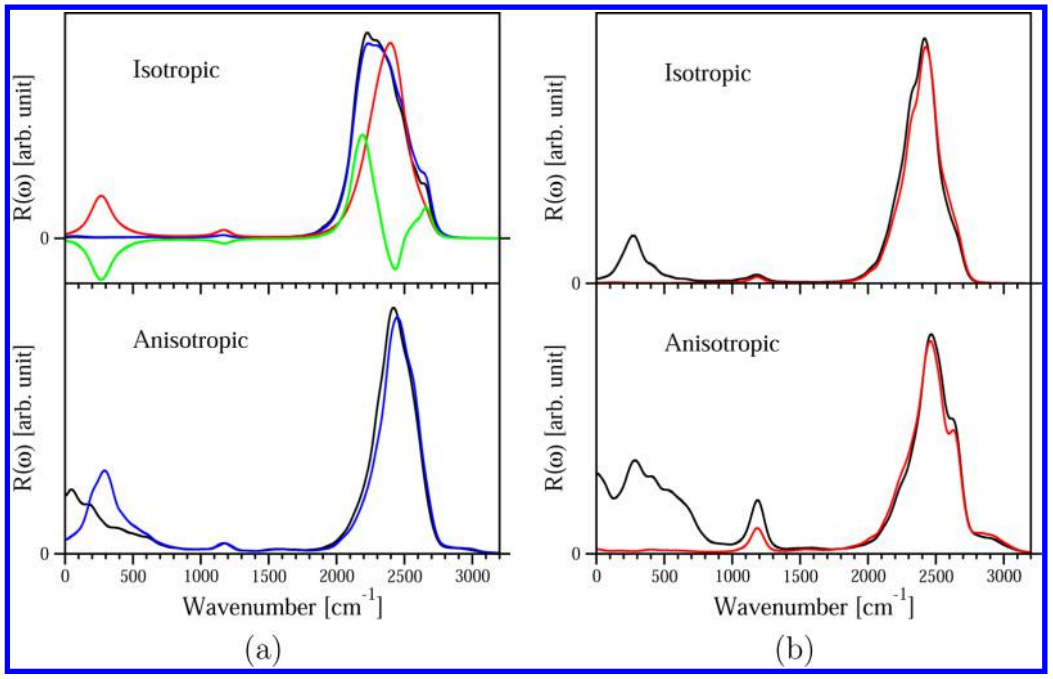

Figure 3. (a) Isotropic (upper panel) and anisotropic (lower panel) Raman spectra (scaled; black lines) compared with the spectra computed from molecular polarizabilities α_i (blue lines) and their intra- (red lines) and inter- (green lines) molecular contributions (see the text). (b) Raman spectra arising from the α_i (black lines) and from α_i' (polarizability of a single, isolated water molecule at the geometry of the molecule in the liquid (see text); red lines).

first principles results may be useful for tuning the parameters of polarizable water models, although absolute values of polarizabilities should probably be obtained using hybrid functionals.[84]

We now turn to analyzing the contribution of molecular polarizabilities to Raman intensities. We compared our results with the total Raman spectra, as shown in Figure 3a. The difference between the two spectra represents the environmental contribution of the polarizability α_i^{DID}. The α_i contribution is approximately proportional to the total Raman spectra in the bending and stretching regions over 1000 cm^{-1}; however, it differs substantially from the total one below this frequency. This can be understood by observing (see eqs 3, 4, S13, and S14) that the difference between α_i^{eff} and α_i is a function of intermolecular distances, r_{ij} (eq S14, SI). At high frequencies, r_{ij} can be assumed constant since water molecules move much slower than the O−D stretching motions, and α_i is therefore proportional to α_i^{eff}. At low frequencies, however, r_{ij} may not be assumed constant, and the DID interactions induced by the collective molecular motions contribute to the difference between the spectra computed from α_i^{eff} or α_i. This analysis suggests that the practice of assuming constant molecular polarizabilities of molecules, as in previous studies[26,30,31,33,34] of Raman spectra, may yield good predictions in the high-frequency stretching region but rather inaccurate results for the low-frequency bands.

The low-frequency part of the anisotropic α_i spectrum (Figure 3a) is particularly interesting. It shows a peak at ∼300 cm^{-1}, that is, in the same region where we identified intermolecular charge fluctuations. In fact, charge fluctuations are a major contribution to this peak, as charge transfer between molecules is responsible for a change of α_i, a mere molecular property. As shown in Figure 3a, the intra- and intermolecular contributions of the isotropic α_i spectrum also show an anticorrelation behavior, proving that the feature identified in the Raman spectra at 270 cm^{-1} does not arise solely from environmental effects (DID interactions), but from the fluctuation of molecular polarizabilities induced by intermolecular charge fluctuations. The peak at 200 cm^{-1} in the anisotropic Raman spectrum is instead a combination of intermolecular charge fluctuations, which contributes to α_i, and of environmental effects. Since no feature is present in the α_i spectrum at 60 cm^{-1}, we conclude that the peak at this frequency mostly originates from DID interactions, which correspond to collective motions of the system.

In order to understand how molecular polarizabilities are modified by the environment in the liquid, we computed the polarizabilities of a single isolated water molecule at the geometry of the molecule in the liquid. We call such polarizability α_i'. Therefore, the difference between α_i' and α_i accounts for the difference in electronic structure induced by the environment. Because of the high computational cost, we calculated α_i' for several but not all water molecules in our simulation, and we computed the α_i' spectra by replacing α by α_i' in eqs 1 and 2. In Figure 3b, we show the comparison of the α_i and α_i' spectra for only one of the water molecules in our sample. While the two spectra agree well in the high-frequency O−D stretching region, we observed clear differences in the low-frequency region. The difference between the two spectra is therefore caused by the change of the electronic structure of the water molecules by the environment in the liquid, namely by intermolecular charge fluctuations.

SUMMARY AND CONCLUSIONS

In summary, we computed the Raman spectra of liquid heavy water from *ab initio* MD simulations using DFPT. These calculations represent the first *ab initio* study of the Raman spectrum of a molecular liquid. Our results are in good agreement with experiments, especially in the low-frequency region of the anisotropic spectrum. We analyzed the Raman

spectra by decomposing the intensities into intra- and intermolecular contributions using MLWFs. In the case of the high-frequency O−D stretching band of the isotropic spectrum, our findings indicate that the intense feature found experimentally at 2500 cm^{-1} arises from intramolecular vibrations, while the one at 2400 cm^{-1} stems from intermolecular coupling; the higher frequency shoulder at 2700 cm^{-1} originates from NHB species, with both inter- and intramolecular contributions. Overall, our results for the high frequency band are consistent with previous studies.[37,38]

In the low-frequency part of the Raman spectra, we identified the presence of intermolecular charge fluctuations at 270 cm^{-1}, accompanying intermolecular HB stretching modes. To support such an identification, we combined a decomposition analysis in terms of intra- and intermolecular contributions, with that of the spread of MLWFs and of molecular polarizabilities. In the anisotropic Raman spectrum, we found that the peak at 200 cm^{-1} has an intermolecular nature and it originates partly from the charge fluctuations and partly from environmental effects. The peak at 60 cm^{-1} is instead due to intramolecular modes determined by DID interactions.

Overall, our simulations showed the importance of *ab initio* methods to accurately describe and interpret the Raman spectra of liquid water, especially in the low-frequency region where intermolecular charge fluctuations are involved.

Following previous studies,[55−57] we defined the molecular polarizabilities of water molecules in the liquid, and we found that its average value is the same in the liquid and in an isolated molecule, while the polarizability anisotropy of water molecules is enhanced in the liquid. These results may be helpful for the parametrization of polarizable force fields of liquid water. We also investigated the contributions of the molecular polarizability α_i to the total Raman spectra and compared it with the spectra computed using α_i', that is, the polarizability of water molecules extracted from the liquid with their geometry kept unchanged. The comparison showed that using constant polarizabilities (or α_i' to replace α_i) in computing Raman spectra, as in many classical simulations,[26,30,31,33−35] may be a good approximation for predicting the stretching band of the Raman spectra but not for the low-frequency region.

Our simulation elucidated the role of intermolecular charge fluctuations in the low-frequency Raman spectra and provided a comprehensive interpretations of the spectra in this region. We note that our *ab initio* methods to calculate and interpret the Raman spectra can be readily used to study aqueous solutions and in general other nonmetallic systems. In addition, only simple modifications are needed to extend our methods to study other vibrational probes such as the surface specific sum frequency vibrational spectroscopy.[89,90]

■ ASSOCIATED CONTENT

Ⓢ Supporting Information

Details about the prefactor in Raman spectra expression, DFPT calculations and the calculation of the effective molecular polarizabilities, molecular polarizabilities, and MLWF spread power spectrum. This material is available free of charge via the Internet at http://pubs.acs.org/.

■ AUTHOR INFORMATION

Corresponding Author

*E-mail: gagalli@ucdavis.edu.

Notes

The authors declare no competing financial interest.

■ ACKNOWLEDGMENTS

We thank D. Pan and C. Zhang for useful discussions. This work was supported by grant DOE-BES DE-SC0008938. Allocation of computing resources by NSF XSEDE through the awards TG-ASC090004 and TG-MCA06N063 are gratefully acknowledged. An award of computer time was provided by the DOE Innovative and Novel Computational Impact on Theory and Experiment (INCITE) program. This research used resources of the Argonne Leadership Computing Facility at Argonne National Laboratory, which is supported by the Office of Science of the U.S. Department of Energy under contract DE-AC02-06CH11357.

■ REFERENCES

(1) Bakker, H. J.; Skinner, J. L. *Chem. Rev.* **2010**, *110*, 1498−517.
(2) Bakker, H. J. *Chem. Rev.* **2008**, *108*, 1456−1473.
(3) Scherer, J. R.; Go, M. K.; Kint, S. *J. Phys. Chem.* **1974**, *78*, 1304−1313.
(4) Walrafen, G. E.; Fisher, M. R.; Hokmabadi, M. S.; Yang, W.-H. *J. Chem. Phys.* **1986**, *85*, 6970.
(5) Brooker, M. H.; Hancock, G.; Rice, B. C.; Shapter, J. *J. Raman Spectrosc.* **1989**, *20*, 683−694.
(6) Zhelyaskov, V.; Georgiev, G.; Nickolov, Z.; Miteva, M. *J. Raman Spectrosc.* **1989**, *20*, 67−75.
(7) Hare, D. E.; Sorensen, C. M. *J. Chem. Phys.* **1992**, *96*, 13.
(8) Carey, D. M.; Korenowski, G. M. *J. Chem. Phys.* **1998**, *108*, 2669.
(9) Galvin, M.; Zerulla, D. *Chem. Phys. Chem.* **2011**, *12*, 913−4.
(10) Paolantoni, M.; Sassi, P.; Morresi, A.; Santini, S. *J. Chem. Phys.* **2007**, *127*, 024504.
(11) Fukasawa, T.; Sato, T.; Watanabe, J.; Hama, Y.; Kunz, W.; Buchner, R. *Phys. Rev. Lett.* **2005**, *95*, 1−4.
(12) Amo, Y.; Tominaga, Y. *Physica A* **2000**, *276*, 401−412.
(13) Winkler, K.; Lindner, J.; Vöhringer, P. *Phys. Chem. Chem. Phys.* **2002**, *4*, 2144−2155.
(14) Castner, E. W.; Chang, Y. J.; Chu, Y. C.; Walrafen, G. E. *J. Chem. Phys.* **1995**, *102*, 653.
(15) Walrafen, G. E. *J. Phys. Chem.* **1990**, *94*, 2237−2239.
(16) Mizoguchi, K.; Hori, Y.; Tominaga, Y. *J. Chem. Phys.* **1992**, *97*, 1961.
(17) Walrafen, G. E.; Hokmabadi, M. S.; Yang, W. H.; Chu, Y. C.; Monosmith, B. *J. Phys. Chem.* **1989**, *93*, 2909−2917.
(18) Goncharov, A.; Goldman, N.; Fried, L.; Crowhurst, J.; Kuo, I.-F.; Mundy, C.; Zaug, J. *Phys. Rev. Lett.* **2005**, *94*, 1−4.
(19) Lin, J.-F.; Gregoryanz, E.; Struzhkin, V. V.; Somayazulu, M.; Mao, H.-k.; Hemley, R. J. *GeoPhys. Res. Lett.* **2005**, *32*, 2−5.
(20) Kawamoto, T.; Ochiai, S.; Kagi, H. *J. Chem. Phys.* **2004**, *120*, 5867−70.
(21) Walrafen, G. E.; Chu, Y. C.; Piermarini, G. J. *J. Phys. Chem.* **1996**, *100*, 10363−10372.
(22) Chumaevskii, N. A.; Rodnikova, M. N. *J. Mol. Liq.* **2002**, *96−97*, 31−43.
(23) Baumgartner, M.; Bakker, R. J. *Mineral. Petrol.* **2008**, *95*, 1−15.
(24) Li, R.; Jiang, Z.; Guan, Y.; Yang, H.; Liu, B. *J. Raman Spectrosc.* **2009**, *40*, 1200−1204.
(25) Heisler, I. a.; Meech, S. R. *Science* **2010**, *327*, 857−60.
(26) Lupi, L.; Comez, L.; Paolantoni, M.; Fioretto, D.; Ladanyi, B. M. *J. Phys. Chem.. B* **2012**, *116*, 7499−508.
(27) Paolantoni, M.; Lago, N. F.; Albert, M.; Laganà, A. *J. Phys. Chem. A* **2009**, *113*, 15100−5.
(28) Alabarse, F. G.; Haines, J.; Cambon, O.; Levelut, C.; Bourgogne, D.; Haidoux, A.; Granier, D.; Coasne, B. *Phys. Rev. Lett.* **2012**, *109*, 035701.
(29) Suzuki, H.; Matsuzaki, Y.; Muraoka, A.; Tachikawa, M. *J. Chem. Phys.* **2012**, *136*, 234508.

(30) Madden, P.; Impey, R. *Chem. Phys. Lett.* **1986**, *123*, 502−506.
(31) Mazzacurati, V.; Ricci, M.; Ruocco, G.; Sampoli, M. *Chem. Phys. Lett.* **1989**, *159*, 383−387.
(32) Bursulaya, B. D.; Kim, H. J. *J. Chem. Phys.* **1998**, *109*, 4911.
(33) Skaf, M.; Sonoda, M. *Phys. Rev. Lett.* **2005**, *94*, 137802.
(34) Sonoda, M. T.; Vechi, S. M.; Skaf, M. S. *Phys. Chem. Chem. Phys.* **2005**, *7*, 1176−80.
(35) Torii, H. *J. Phys. Chem. A* **2006**, *110*, 9469−77.
(36) Loparo, J. J.; Roberts, S. T.; Nicodemus, R. a.; Tokmakoff, A. *Chem. Phys.* **2007**, *341*, 218−229.
(37) Auer, B. M.; Skinner, J. L. *J. Chem. Phys.* **2008**, *128*, 224511.
(38) Yang, M.; Skinner, J. L. *Phys. Chem. Chem. Phys.* **2010**, *12*, 982−91.
(39) McQuarrie, D. A. *Statistical Mechanics*; University Science Books: Henderson, VA, 2000; pp 484−489.
(40) Ramírez, R.; López-Ciudad, T.; Kumar, P, P.; Marx, D. *J. Chem. Phys.* **2004**, *121*, 3973−83.
(41) Padro, J. A.; Marti, J. *J. Chem. Phys.* **2003**, *118*, 452−453.
(42) De Santis, A.; Ercoli, A.; Rocca, D. *J. Chem. Phys.* **2004**, *120*, 1657−8.
(43) Padro, J. A.; Marti, J. *J. Chem. Phys.* **2004**, *120*, 1659.
(44) Sharma, M.; Resta, R.; Car, R. *Phys. Rev. Lett.* **2005**, *95*, 187401.
(45) Chen, W.; Sharma, M.; Resta, R.; Galli, G.; Car, R. *Phys. Rev. B* **2008**, *77*, 245114.
(46) Zhang, C.; Donadio, D.; Galli, G. *J. Phys. Chem. Lett.* **2010**, *1*, 1398−1402.
(47) Baroni, S.; De Gironcoli, S.; Dal Corso, A.; Giannozzi, P. *Rev. Mod. Phys.* **2001**, *73*, 515.
(48) Putrino, A.; Parrinello, M. *Phys. Rev. Lett.* **2002**, *88*, 176401.
(49) Pagliai, M.; Cavazzoni, C.; Cardini, G.; Erbacci, G.; Parrinello, M.; Schettino, V. *J. Chem. Phys.* **2008**, *128*, 224514.
(50) Marzari, N.; Mostofi, A.; Yates, J.; Souza, I.; Vanderbilt, D. *Rev. Mod. Phys.* **2012**, *84*, 1419−1475.
(51) Silvestrelli, P. L.; Bernasconi, M.; Parrinello, M. *Chem. Phys. Lett.* **1997**, *277*, 478−482.
(52) Silvestrelli, P.; Parrinello, M. *Phys. Rev. Lett.* **1999**, *82*, 3308−3311.
(53) Pasquarello, A.; Resta, R. *Phys. Rev. B* **2003**, *68*, 174302.
(54) Torii, H. *J. Phys. Chem. B* **2011**, *115*, 6636−43.
(55) Heaton, R. J.; Madden, P. A.; Clark, S. J.; Jahn, S. *J. Chem. Phys.* **2006**, *125*, 144104.
(56) Salanne, M.; Vuilleumier, R.; Madden, P. A.; Simon, C.; Turq, P.; Guillot, B. *J. Phys.: Condens. Matter* **2008**, *20*, 494207.
(57) Buin, A.; Iftimie, R. *J. Chem. Phys.* **2009**, *131*, 234507.
(58) Molina, J. J.; Lectez, S.; Tazi, S.; Salanne, M.; Dufrêche, J.-F.; Roques, J.; Simoni, E.; Madden, P. a.; Turq, P. *J. Chem. Phys.* **2011**, *134*, 014511.
(59) *Qbox Code*. http://eslab.ucdavis.edu/software/qbox/ (accessed July 18, 2013).
(60) Perdew, J.; Burke, K.; Ernzerhof, M. *Phys. Rev. Lett.* **1996**, *77*, 3865−3868.
(61) Zhang, C.; Donadio, D.; Galli, G.; Gygi, F. *J. Chem. Theory Comput.* **2011**, *7*, 1443−1449.
(62) Hamann, D.; Schlüter, M.; Chiang, C. *Phys. Rev. Lett.* **1979**, *43*, 1494−1497.
(63) Vanderbilt, D. *Phys. Rev. B* **1985**, *32*, 8412−8415.
(64) Bussi, G.; Donadio, D.; Parrinello, M. *J. Chem. Phys.* **2007**, *126*, 014101.
(65) Gygi, F.; Fattebert, J.-L.; Schwegler, E. *Comput. Phys. Commun.* **2003**, *155*, 1−6.
(66) Faurskov Nielsen, O. *Annu. Rep. Prog. Chem., Sect. C: Phys. Chem.* **1997**, *93*, 57.
(67) Nakayama, T. *Phys. Rev. Lett.* **1998**, *80*, 1244−1247.
(68) Torii, H. *Chem. Phys. Lett.* **2002**, *353*, 431−438.
(69) Zhang, C.; Wu, J.; Galli, G.; Gygi, F. F. *J. Chem. Theory Comput.* **2011**, *7*, 3054.
(70) Eaves, J.; Loparo, J. *Proc. Natl. Acad. Sci. U.S.A.* **2005**, *102*, 13019−13022.
(71) Cappelletti, D.; Ronca, E.; Belpassi, L.; Tarantelli, F.; Pirani, F. *Acc. Chem. Res.* **2012**, *45*, 1571−80.
(72) Ghanty, T. K.; Staroverov, V. N.; Koren, P. R.; Davidson, E. R. *J. Am. Chem. Soc.* **2000**, *122*, 1210−1214.
(73) Glendening, E. D. *J. Phys. Chem. A* **2005**, *109*, 11936−40.
(74) Khaliullin, R. Z.; Bell, A. T.; Head-Gordon, M. *Chem.—Eur. J.* **2009**, *15*, 851−855.
(75) Stone, A. J.; Misquitta, A. J. *Chem. Phys. Lett.* **2009**, *473*, 201−205.
(76) Chelli, R.; Schettino, V.; Procacci, P. *J. Chem. Phys.* **2005**, *122*, 234107.
(77) Berendsen, H. J. C.; Grigera, J. R.; Straatsma, T. P. *J. Phys. Chem.* **1987**, *91*, 6269−6271.
(78) Chatterjee, S.; Debenedetti, P. G.; Stillinger, F. H.; Lynden-Bell, R. M. *J. Chem. Phys.* **2008**, *128*, 124511.
(79) Jorgensen, W. L.; Chandrasekhar, J.; Madura, J. D.; Impey, R. W.; Klein, M. L. *J. Chem. Phys.* **1983**, *79*, 926.
(80) Lee, A. J.; Rick, S. W. *J. Chem. Phys.* **2011**, *134*, 184507.
(81) Lee, A. J.; Rick, S. W. *J. Phys. Chem. Lett.* **2012**, *3*, 3199−3203.
(82) Soniat, M.; Rick, S. W. *J. Chem. Phys.* **2012**, *137*, 044511.
(83) Porezag, D.; Pederson, M. *Phys. Rev. B* **1996**, *54*, 7830−7836.
(84) Xu, X.; Goddard, W. a. *J. Phys. Chem. A* **2004**, *108*, 2305−2313.
(85) Schropp, B.; Tavan, P. *J. Phys. Chem. B* **2008**, *112*, 6233−40.
(86) Murphy, W. F. *J. Chem. Phys.* **1977**, *67*, 5877.
(87) Lamoureux, G.; MacKerell, A. D.; Roux, B. *J. Chem. Phys.* **2003**, *119*, 5185.
(88) Rick, S. W.; Stuart, S. J.; Berne, B. J. *J. Chem. Phys.* **1994**, *101*, 6141.
(89) Shen, Y. R.; Ostroverkhov, V. *Chem. Rev.* **2006**, *106*, 1140−54.
(90) Perry, A.; Neipert, C.; Space, B.; Moore, P. B. *Chem. Rev.* **2006**, *106*, 1234−58.